MAGMA (2004) 17: 149–156
DOI 10.1007/s10334-004-0066-4

REVIEW ARTICLE

Current status of cardiac MRI in small animals

J.-P. Vallée
M. K. Ivancevic
D. Nguyen
D. R. Morel
M. Jaconi

Received: 2 July 2004
Revised: 27 August 2004
Accepted: 15 September 2004
Published online: 16 December 2004

J.-P. Vallée (✉) · M. K. Ivancevic
D. Nguyen
Digital Imaging Unit,
Radiology and Medical Informatics
Department, Geneva University Hospitals
CH-1211 Geneva 14,
Switzerland
E-mail: jean-paul.vallee@sim.hcuge.ch

D. R. Morel
Investigations Anesthésiologiques,
APSIC Department,
Geneva University Hospitals,
Switzerland

M. Jaconi
Laboratory of Biology of Aging,
Geriatrics Department,
Geneva University Hospitals,
Switzerland

Abstract Cardiac magnetic resonance imaging (MRI) on small animals is possible but remains challenging and not well standardized. This publication aims to provide an overview of the current techniques, applications and challenges of cardiac MRI in small animals for researchers interested in moving into this field. Solutions have been developed to obtain a reliable cardiac trigger in both the rat and the mouse. Techniques to measure ventricular function and mass have been well validated and are used by several research groups. More advanced techniques like perfusion imaging, delayed enhancement or tag imaging are emerging. Regarding cardiac applications, not only coronary ischemic disease but several other pathologies or conditions including cardiopathies in transgenic animals have already benefited from these new developments. Therefore, cardiac MRI has a bright future for research in small animals.

Keywords Magnetic resonance imaging · Heart · Coronary ischemic disease · Rat

Introduction

Magnetic resonance imaging (MRI) is a powerful technique used both in clinical practice and in research. In routine cardiac imaging, MRI is recognized as a robust and accurate method to measure cardiac function, perfusion and viability. The ease of transferring new methods developed on experimental models to clinical imaging is another stimulus to perform research on cardiac MRI. Research on small animals has numerous advantages such as realistic physiologic in vivo models, knockout animals as well as reduced team and cost to handle the experiments. Several imaging methods have been developed for the phenotypic analysis of small animals, amongst which MRI has been proposed [1]. Still, cardiac imaging on a small animal using MRI remains challenging and not well standardized. Therefore, this work aims to provide an overview of the current techniques, applications and challenges of cardiac MRI in small animals for researchers interested in moving into this field. First, the methodology will be discussed followed by the applications and results obtained so far.

Cardiac MRI acquisition

Optimal magnetic field strength

Usually, cardiac MRI research is performed on high-field magnets with a small bore specially designed for small animals. The advantage of using high fields relies on the increased signal that allows higher resolution to be achieved. Fields of 4.7 and 7 T are commonly used [2]. Experiences on 11 T and above have also been reported for applications like coronary angiography and phosphorus spectroscopy [2]. The position of the magnet (horizontal vs. vertical as encountered in high-field systems) does not seem to be relevant as prolonged upright body position exerts no significant changes in murine left ventricle hemodynamics [3]. However, high field is not mandatory as successful experiments have also be performed at 1.5 T on a clinical system [4, 5]. The loss of signal is compensated to some extent by dedicated coils that improve the signal reception.

Trigger systems and animal monitoring

For structural studies like myocardial mass quantification, high-quality predominantly diastolic MR images may be obtained by signal averaging without any trigger (6). However, for all other techniques including a fast determination of the myocardial mass, an ECG trigger is absolutely required for cardiac MRI. Considering the high heart rate encountered in small animals (between 200 and 600 bpm) and the small voltage recorded for the ECG, the cardiac synchronization can be really challenging. Commercial trigger systems are available that can amplify the ECG signal recorded in small animals. However, the ECG may be corrupted during image acquisition by the imaging process, as for example in cardiac microscopy when short repetition time and high gradient-slew rate are used. Therefore other types of trigger devices have been developed [7]. The fiber-optic stethoscope system for example is inserted in the esophagus and optically detects pulsate compression of the esophageal wall [8]. As another type of device, the «lever-coil» is a coil mechanically coupled to the animal but not located within the resonator or gradient coil that is sensitive to both cardiac and respiratory motion [9]. Finally, the arterial pressure can also be used to trigger the MRI acquisition instead of the ECG [10].

Regarding the need for a respiratory gating, the position of the animal seems important as respiratory compensation is needed in vertical high-field magnets but not in horizontal magnets [11].

In addition to image triggering, cardiac and respiratory monitoring permits the display of vital signs. In conjunction with general anesthesia under isoflurane [12] and body temperature control [13], exam durations of around 2 h have been achieved.

MR sequences and protocols

Various sequences are used for cardiac imaging in rats (10). There are no systematic studies comparing the different MR sequences. The choice of the MR sequences seems to depend more on both the investigators and the MR systems used. The most frequently used are T1 gradient echo cine sequences, yielding a typical in-plane resolution of 200–300 μm in less than a minute for a single slice on high-field magnets [14].

Myocardial mass

Due to its ability to offer high spatial resolution, myocardial mass can be accurately quantified in vivo by MRI, as it has been demonstrated in the mouse [15–17]. The method relies on a complete coverage of the heart using cine images, followed by a delineation of the epicardial and endocardial contours of the left ventricle, as shown on Fig. 1. By considering the cardiac tissue density as constant, the segmented volume yields the mass.

This method has been validated by left-ventricle gravimetry [16]. Additional parameters like the volume of the cavities or the slice thickness can also be measured from the images.

On an isolated beating heart and high-field MR systems, the spatial resolution can be increased to observe the myocardial fiber structure [18–20]. Diffusion imaging has also been performed on isolated beating [19] and fixed hearts [21].

Myocardial function

One of the strengths of cardiac MRI is the accuracy of measuring myocardial function in small animals. Several protocols have been proposed according to the type of measurements needed.

Global and regional function

Global and regional functions are obtained using bright blood cine-imaging MR sequences [11, 22]. Parameters like ejection fraction, or wall thickness and wall thickening are reproducibly extracted from these data based on the high contrast between the blood and the myocardium. Stress cine-MRI of cardiac function have been performed using dobutamine in mice with an intravenous infusion at 4 or 40 μg/minute/kg [23], or an intra-peritoneal bolus injection of 1.5 μg/g body weight [24, 25].

Strain and velocity imaging

Intra-myocardial wall motion, like radial and circumferential shortening or strains, torsion angle, can be measured

on strain imaging but not on cine imaging. The basic principle is to tag the myocardium physically using spatially selective saturation pulses and to track the displacement of the tagged myocardium. The feasibility of such an approach has already been demonstrated in the mouse using either SPAMM or DENSE imaging, as shown in Fig. 2 [26–30]. Another variant of these approaches uses phase-contrast imaging with bipolar gradients to encode the motion of the mouse myocardium [31]. The different merits and respective indications of these three techniques are yet to be determined in small animals.

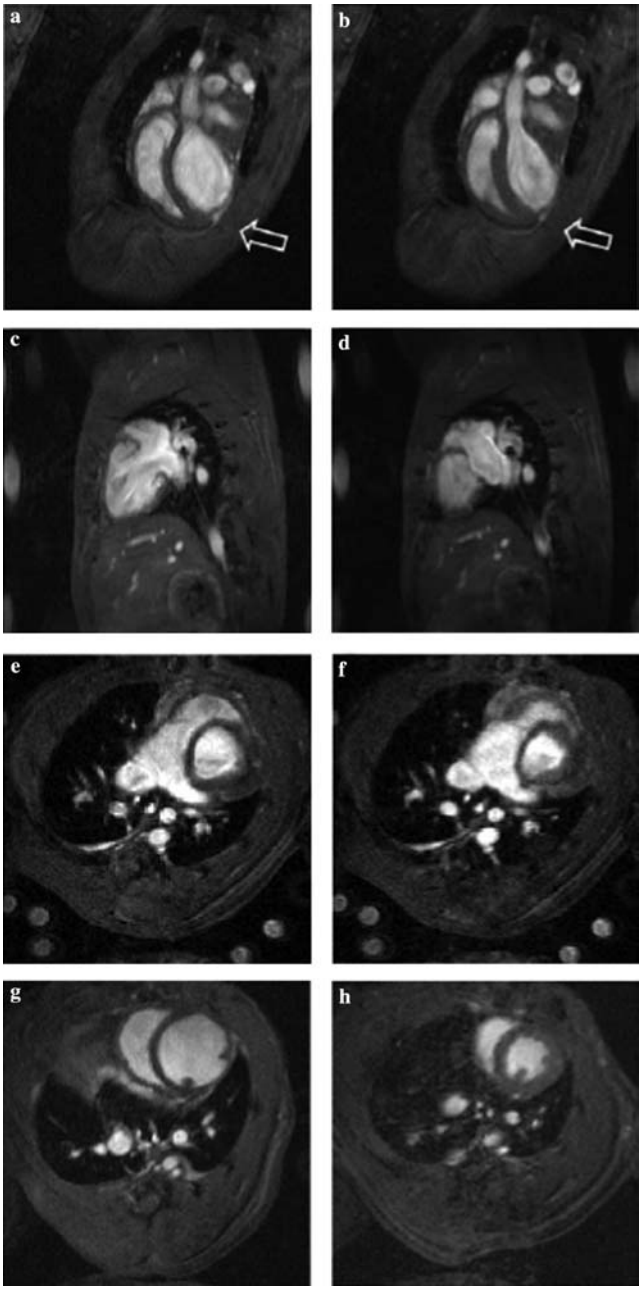

Fig. 1 **a** and **b**: long-axis view of a rat heart 8 wk after large myocardial infarction (MI) in diastole (**a**) and systole (**b**). **c** and **d**: long-axis views of the RV 8 week after large MI in diastole (**c**) and systole (**d**). **e** and **f**: diastolic (**e**) and systolic (**f**) short-axis slices at the level of the tricuspid valve in a rat 8 wk after MI. **g** and **h**: diastolic short-axis slices at the level of the papillary muscles in a rat 8 wk after MI (**g**) and a sham-operated rat (**h**). Note the high spatial resolution that allows a clear delineation of the cardiac anatomy and to differential the normal and infarcted heart.(reprinted with permission form reference [65])

Myocardial perfusion and blood volume

Quantification of coronary blood flow using phase-contrast techniques in small animals has only been achieved on isolated hearts [32]. Research has been more focused on measuring perfusion at the tissue level. Spin-labeling perfusion techniques [33] have been used in small animals [34–38] as an endogenous alternative to the myocardial perfusion measurement with exogenous contrast media used in humans. Indeed, in humans cardiac frequency is low enough to allow the acquisition of images with sufficient SNR and resolution within one heart beat to follow bolus. In small rodents, however, cardiac cycle duration is much shorter, of the order of 100–200 ms. This precludes acquisition of images with sufficient resolution and SNR within one heart beat. Therefore, MRI bolus tracking is less reliable in small animals. Also, reproducible bolus injections, required for perfusion quantification, are difficult to achieve in small animals [39].

The principle of spin-labeling perfusion quantification is based on inflowing, non-inverted spins into a selectively inverted slice. The mixing of non-inverted flowing and inverted spins in the imaging slice modifies the apparent relaxation time and thus creates flow-related contrast. Since T1 increases with higher magnetic fields, and higher T1 values allow longer inflow observation times, high magnetic fields are particularly useful for spin-labeling imaging.

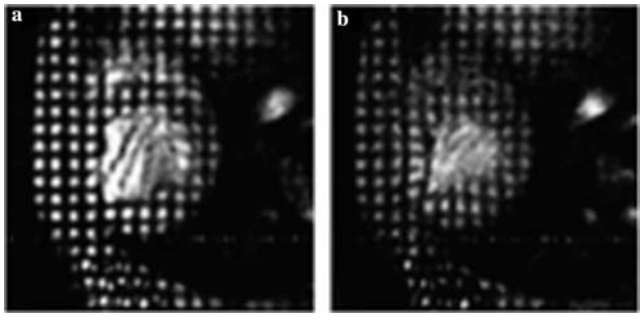

Fig. 2 Typical images from an 11-phase (time points) tag MRI study in mouse are depicted shortly after end diastole (**a**) and at end systole (**b**). The analysis of the tag displacement is used to measure myocardial strains. (adapted with permission from reference [29])

Myocardial perfusion values at rest in rats from $3.5 \pm 0.1\,mg\,g^{-1}\,min^{-1}$ [35] to $5.5 \pm 0.7\,mg\,g^{-1}\,min^{-1}$ [34] have been reported in the literature and validated using a colored microspheres technique [35].

In addition to perfusion measurement by spin tagging, the injection of a T1 intravascular contrast media allows the determination of the myocardial blood volume [35, 40]. Other methods to measure regional myocardial blood volume is based on the accepted linear relationship between the regional blood volume and the transverse relaxation rate increase, $\Delta R2^*$, following iron oxide particle injection [41].

Delayed enhancement MRI

Delayed imaging after contrast media injection is an established MR technique to reveal acute or chronic infarct in patients. This technique has been well validated in the mouse with an occlusion/reperfusion model and an extravascular contrast media (Gd-DTPA at a dose of 0.3–0.6 mmol/kg) by comparison to TTC staining [42]. In the rat with the occlusion/reperfusion model, however, the situation is less clear with more debated results. Both intravascular [43] and extravascular contrast media overestimated the infarct size whereas necrosis-avid gadolinium-based contrast media gave a correct measure [44]. In another rat study with a similar model, the enhanced region overestimated the infarct size immediately after the injection of Gd-DTPA, although it gradually decreased to match the size of the infarct [45]. Such a variation of the hyperenhanced region is not found in patients or other models and needs to be further studied [46].

Manganese-based contrast media have also been used to delineate myocardial infarct in rats as they accumulate inside normal myocytes but not in infarcted cells [47, 48]. However, the practical use of such contrast media that may also indicate the rate of calcium influx into the heart [25] remains to be defined.

Metabolism and spectroscopy

The feasibility of 31 P MR spectroscopy has already been demonstrated in mice on isolated hearts [49, 50] and in vivo [51]. Using this technique, the myocardial phosphocreatine (PCr)-to-ATP (PCr/ATP) ratio remained unchanged in mice after dobutamine stress [49]. A report on sodium MR imaging in isolated rat hearts demonstrated an increase of the intracellular sodium during global ischemia [52]. However, these techniques remain difficult to master and are not widely used.

Angiography and vessel wall imaging

Coronary MR angiography has been successfully performed on isolated rat hearts to demonstrate a coronary occlusion [2] but remains technically difficult, although possible, in mice in vivo [53]. Wall imaging of mice artery is a rapidly growing field due to the numerous knockout models that are available. With this technique, high MRI resolution of a limited vessel segment has been acquired in vivo in the aorta and carotid arteries of mice [54–59]. There are currently no reports on wall imaging of coronary arteries in small animals.

Cardiac MRI applications

Using the previously described protocols on small animals, significant results have already been obtained in the cardiovascular field. These will be briefly reviewed to demonstrate the potential of cardiac MRI in small animals.

Persistent coronary occlusion

This model is characterized by a permanent occlusion of a coronary artery, yielding an infarct of variable size depending on the site of the ligation (distal or proximal) [60]. The remodeling following myocardial infarct in the left ventricle has been well described using MRI [61]: the injured myocardium evolves toward scar tissue and the remote myocardium develops a hypertrophy of the wall as well as an increase of the intracapillary blood volume [62]. Ultimately, a cardiac failure may result [63]. MRI also demonstrated a right ventricle hypertrophy as in the left ventricle but no increase of the wall stress [64, 65].

The effect of transmyocardial laser revascularization [66], angiotensin converting enzyme inhibitors [67], testosterone [68] or statin [69] in this model of myocardial infarction have also been investigated.

Occlusion/reperfusion model

This model is characterized by a transitory occlusion of a coronary artery, usually at its origin, followed by a release of the occlusion insuring a reperfusion of the injured myocardium. This results in an ischemia or an infarct of variable size depending of the duration of the occlusion. It allows also to study the no-reflow phenomenon characterized by obstructed intramyocardial micro-vessels despite reopened epicardial arteries [70].

MRI has been used to assess both infarct size and cardiac function in intact mice early after a large, reperfused myocardial infarction, revealing the existence of contractile dysfunction in non-infarcted regions of the heart [30, 70]. Nicorandil, a K-ATP channel opener with a nitrate-like effect attenuates left-ventricular dilatation and improves cardiac function in rats with reperfused myocardial infarction, as demonstrated by MRI [71–73]. In transgenic

mice with the occlusion/reperfusion model, MRI demonstrated the beneficial effect of over-expression of A1-adenosine receptors [74] and Angiotensin II type 2 receptors [75] on both systolic function and infarct size.

Partial coronary occlusion (chronic ischemia)

In this model, a subtotal occlusion of the coronary artery results in impaired cardiac function and anatomy with multiple sites of injury including myocyte loss and hypertrophy and reparative fibrosis [76]. The effect of partial coronary occlusion on the residual myocardial blood flow at rest is controversial as it was found normal when measured by microspheres [77] but decreased in a recent study using MRI [78]. Perfusion, function and energy metabolism as assayed by 31 P spectroscopy in this model have been successfully obtained by MRI [2]. Although less often studied than the two previous models, the partial coronary occlusion technique has a strong potential as it can mimic the ischemic cardiopathy encountered in man.

Other models

As the MRI technique to measure the cardiac function and mass is now validated for mice, numerous MR studies have been performed using transgenic animals such as myoglobin knockout mice [79], VEGF knockout mice [23], apolipoprotein E-deficient mice [80], caveoline-deficient mice [81] and transgenic mice expressing tumor necrosis factor alpha (TNF-alpha) [4].

Hyperthyroid and hypertensive cardiomyopathies have been studied by MRI. It was observed that the continuous blockade of calcium channels suppresses activation of calcineurin and the development of cardiac hypertrophy in spontaneously hypertensive rats [82, 83]. Mice with cardiomyocyte-specific disruption of the endothelin-1 gene were resistant to hyperthyroid cardiac hypertrophy [5].

MRI demonstrated the reduction of the myocardial mass and the amelioration of cardiac function induced by the angiotensin-converting enzyme (ACE) inhibitor captopril in streptozotocin (STZ)-diabetic male Wistar rats [84, 85].

MRI has also been used to study the cardiac graft rejection [86] with the accumulation of macrophages inside the transplant [87].

Finally, a series of experiments has been conducted to study the treatment and consequences of chagasic heart disease in mice [88–91, 91].

Conclusions

This review illustrates the strong potential of MRI for cardiac imaging of small animals. Solutions have been found to obtain a reliable cardiac trigger in both the rat and the mouse. Techniques to measure ventricular function and mass have been well validated and are used by several research groups. More advanced techniques like perfusion imaging, delayed enhancement or tag imaging are emerging. However, an effort is still needed to standardize the acquisition protocols and data analysis. In this respect, better gold standards of cardiac parameters are required. For example, an atlas of normal and pathological cardiac strains as measured by tag MRI would be particularly useful. Regarding the cardiac application, not only coronary ischemic disease but several other pathologies including transgenic animals have already benefited from these new developments. Therefore, cardiac MRI has a bright future for research in small animals.

Acknowledgements Swiss National Science Foundation (PPOOB-68778 and NRP-4046-058712) and the Radiology and Medical Informatics Department.

References

1. Hoit BD (2001) New approaches to phenotypic analysis in adult mice. J Mol Cell Cardiol 33:27–35
2. Nahrendorf M, Hiller KH, Greiser A, Kohler S, Neuberger T, Hu K, Waller C et al (2003) Chronic coronary artery stenosis induces impaired function of remote myocardium: MRI and spectroscopy study in rat. Am J Physiol Heart Circ Physiol 285:H2712–2721
3. Wiesmann F, Neubauer S, Haase A, Hein L (2001) Can we use vertical bore magnetic resonance scanners for murine cardiovascular phenotype characterization? Influence of upright body position on left ventricular hemodynamics in mice. J Cardiovasc Magn Reson 3:311–315
4. Franco F, Thomas GD, Giroir B, Bryant D, Bullock MC, Chwialkowski MC, Victor RG et al. (1999) Magnetic resonance imaging and invasive evaluation of development of heart failure in transgenic mice with myocardial expression of tumor necrosis factor-alpha. Circulation 99:448–454

5. Shohet RV, Kisanuki YY, Zhao XS, Siddiquee Z, Franco F, Yanagisawa M (2004) Mice with cardiomyocyte-specific disruption of the endothelin-1 gene are resistant to hyperthyroid cardiac hypertrophy. Proc Natl Acad Sci USA 101:2088–2093
6. Rudin M, Allegrini PR, Beckmann N, Ekatodramis D, Laurent D (2000) In-vivo cardiac studies in animals using magnetic resonance techniques: experimental aspects and MR readouts. MAGMA 11:33–35
7. Cassidy PJ, Schneider JE, Grieve SM, Lygate C, Neubauer S, Clarke K (2004) Assessment of motion gating strategies for mouse magnetic resonance at high magnetic fields. J Magn Reson Imaging 19:229–237
8. Brau AC, Wheeler CT, Hedlund LW, Johnson GA (2002) Fiber-optic stethoscope: a cardiac monitoring and gating system for magnetic resonance microscopy. Magn Reson Med 47:314–321
9. Fishbein KW, McConville P, Spencer RG (2001) The lever-coil: a simple, inexpensive sensor for respiratory and cardiac motion in MRI experiments. Magn Reson Imaging 19:881–889
10. Rehwald WG, Reeder SB, McVeigh ER, Judd RM (1997) Techniques for high-speed cardiac magnetic resonance imaging in rats and rabbits. Magn Reson Med 37:124–130
11. Schneider JE, Cassidy PJ, Lygate C, Tyler DJ, Wiesmann F, Grieve SM, Hulbert K et al. (2003) Fast, high-resolution in vivo cine magnetic resonance imaging in normal and failing mouse hearts on a vertical 11.7 T system. J Magn Reson Imaging 18:691–701
12. Wood AK, Klide AM, Pickup S, Kundel HL (2001) Prolonged general anesthesia in MR studies of rats. Acad Radiol 8:1136–1140
13. Qiu HH, Cofer GP, Hedlund LW, Johnson GA (1997) Automated feedback control of body temperature for small animal studies with MR microscopy. IEEE Trans Biomed Eng 44:1107–1113
14. Nahrendorf M, Wiesmann F, Hiller KH, Hu K, Waller C, Ruff J, Lanz TE et al. (2001) Serial cine-magnetic resonance imaging of left ventricular remodeling after myocardial infarction in rats. J Magn Reson Imaging 14:547–555
15. Ruff J, Wiesmann F, Hiller KH, Voll S, von Kienlin M, Bauer WR, Rommel E et al. (1998) Magnetic resonance microimaging for noninvasive quantification of myocardial function and mass in the mouse. Magn Reson Med 40:43–48
16. Siri FM, Jelicks LA, Leinwand LA, Gardin JM (1997) Gated magnetic resonance imaging of normal and hypertrophied murine hearts. Am J Physiol 272:H2394–2402
17. Slawson SE, Roman BB, Williams DS, Koretsky AP (1998) Cardiac MRI of the normal and hypertrophied mouse heart. Magn Reson Med 39:980–987
18. Kohler S, Hiller KH, Griswold M, Bauer WR, Haase A, Jakob PM (2003) NMR-microscopy with TrueFISP at 11.75 T. J Magn Reson 161:252–257
19. Kohler S, Hiller KH, Waller C, Bauer WR, Haase A, Jakob PM (2003) Investigation of the microstructure of the isolated rat heart: a comparison between T*2- and diffusion-weighted MRI. Magn Reson Med 50:1144–1150
20. Kohler S, Hiller KH, Waller C, Jakob PM, Bauer WR, Haase A (2003) Visualization of myocardial microstructure using high-resolution T*2 imaging at high magnetic field. Magn Reson Med 49:371–375
21. Chen J, Song SK, Liu W, McLean M, Allen JS, Tan J, Wickline SA et al. (2003) Remodeling of cardiac fiber structure after infarction in rats quantified with diffusion tensor MRI. Am J Physiol Heart Circ Physiol 285:H946–954
22. Ross AJ, Yang Z, Berr SS, Gilson WD, Petersen WC, Oshinski JN, French BA (2002) Serial MRI evaluation of cardiac structure and function in mice after reperfused myocardial infarction. Magn Reson Med 47:1158–1168
23. Williams SP, Gerber HP, Giordano FJ, Peale FV, Jr., Bernstein LJ, Bunting S, Chien KR et al. (2001) Dobutamine stress cine-MRI of cardiac function in the hearts of adult cardiomyocyte-specific VEGF knockout mice. J Magn Reson Imaging 14:374–382
24. Wiesmann F, Ruff J, Engelhardt S, Hein L, Dienesch C, Leupold A, Illinger R et al. (2001) Dobutamine-stress magnetic resonance microimaging in mice: acute changes of cardiac geometry and function in normal and failing murine hearts. Circ Res 88:563–569
25. Hu TC, Pautler RG, MacGowan GA, Koretsky AP (2001) Manganese-enhanced MRI of mouse heart during changes in inotropy. Magn Reson Med 46:884–890
26. Henson RE, Song SK, Pastorek JS, Ackerman JJ, Lorenz CH (2000) Left ventricular torsion is equal in mice and humans. Am J Physiol Heart Circ Physiol 278:H1117–H1123
27. Wu EX, Towe CW, Tang H (2002) MRI cardiac tagging using a sinc-modulated RF pulse train. Magn Reson Med 48:389–393
28. Zhou R, Pickup S, Glickson JD, Scott CH, Ferrari VA (2003) Assessment of global and regional myocardial function in the mouse using cine and tagged MRI. Magn Reson Med 49:760–764
29. Gilson WD, Yang Z, French BA, Epstein FH (2004) Complementary displacement-encoded MRI for contrast-enhanced infarct detection and quantification of myocardial function in mice. Magn Reson Med 51:744–752
30. Epstein FH, Yang Z, Gilson WD, Berr SS, Kramer CM, French BA (2002) MR tagging early after myocardial infarction in mice demonstrates contractile dysfunction in adjacent and remote regions. Magn Reson Med 48:399–403
31. Streif JU, Herold V, Szimtenings M, Lanz TE, Nahrendorf M, Wiesmann F, Rommel E et al. (2003) In vivo time-resolved quantitative motion mapping of the murine myocardium with phase contrast MRI. Magn Reson Med 49:315–321
32. Kohler S, Hiller KH, Jakob PM, Bauer WR, Haase A (2003) Time-resolved flow measurement in the isolated rat heart: characterization of left coronary artery stenosis. Magn Reson Med 50:449–452
33. Williams DS, Detre JA, Leigh JS, Koretsky AP (1992) Magnetic resonance imaging of perfusion using spin inversion of arterial water. Proc Nat Aca Sci U S A 89:212–216
34. Kober F, Iltis I, Izquierdo M, Desrois M, Ibarrola D, Cozzone PJ, Bernard M (2004) High-resolution myocardial perfusion mapping in small animals in vivo by spin-labeling gradient-echo imaging. Magn Reson Med 51:62–67
35. Waller C, Kahler E, Hiller KH, Hu K, Nahrendorf M, Voll S, Haase A et al. (2000) Myocardial perfusion and intracapillary blood volume in rats at rest and with coronary dilatation: MR imaging in vivo with use of a spin-labeling technique. Radiology 215:189–197
36. Belle V, Kahler E, Waller C, Rommel E, Voll S, Hiller KH, Bauer WR et al. (1998) In vivo quantitative mapping of cardiac perfusion in rats using a noninvasive MR spin-labeling method. J Magn Reson Imaging 8:1240–1245

37. Utting JF, Thomas DL, Gadian DG, Ordidge RJ (2003) Velocity-driven adiabatic fast passage for arterial spin labeling: results from a computer model. Magn Reson Med 49:398–401
38. Waller C, Hiller KH, Voll S, Haase A, Ertl G, Bauer WR (2001) Myocardial perfusion imaging using a non-contrast agent MR imaging technique. Int J Cardiovasc Imaging 17:123–132
39. Pickup S, Zhou R, Glickson J (2003) MRI estimation of the arterial input function in mice. Acad Radiol 10:963–968
40. Kahler E, Waller C, Rommel E, Belle V, Hiller KH, Voll S, Bauer WR et al. (1999) Perfusion-corrected mapping of cardiac regional blood volume in rats in vivo. Magn Reson Med 42:500–506
41. Wu EX, Tang H, Wong KK, Wang J (2004) Mapping cyclic change of regional myocardial blood volume using steady-state susceptibility effect of iron oxide nanoparticles. J Magn Reson Imaging 19:50–58
42. Yang Z, Berr SS, Gilson WD, Toufektsian M-C, French BA (2004) Simultaneous evaluation of infarct size and cardiac function in intact mice by contrast-enhanced cardiac magnetic resonance imaging reveals contractile dysfunction in noninfarcted regions early after myocardial infarction. Circulation 109:1161–1167
43. Krombach GA, Wendland MF, Higgins CB, Saeed M (2002) MR imaging of spatial extent of microvascular injury in reperfused ischemically injured rat myocardium: value of blood pool ultrasmall superparamagnetic particles of iron oxide. Radiology 225:479–486
44. Saeed M, Lund G, Wendland MF, Bremerich J, Weinmann H, Higgins CB (2001) Magnetic resonance characterization of the peri-infarction zone of reperfused myocardial infarction with necrosis-specific and extracellular nonspecific contrast media. Circulation 103:871–876
45. Oshinski JN, Yang Z, Jones JR, Mata JF, French BA (2001) Imaging time after Gd-DTPA injection is critical in using delayed enhancement to determine infarct size accurately with magnetic resonance imaging. Circulation 104:2838–2842
46. Judd RM, Kim RJ, Oshinski JN, Yang Z, Jones JR, Mata J, French BA (2002) Imaging time after Gd-DTPA injection is critical in using delayed enhancement to determine infarct size accurately with magnetic resonance imaging * response. Circulation 106:6e
47. Bremerich J, Saeed M, Arheden H, Higgins CB, Wendland MF (2000) Normal and infarcted myocardium: differentiation with cellular uptake of manganese at MR imaging in a rat model. Radiology 216:524–530
48. Wyttenbach R, Saeed M, Wendland MF, Geschwind JF, Bremerich J, Arheden H, Higgins CB (1999) Detection of acute myocardial ischemia using first-pass dynamics of MnDPDP on inversion recovery echoplanar imaging. J Magn Reson Imaging 9:209–214
49. Chacko VP, Aresta F, Chacko SM, Weiss RG (2000) MRI/MRS assessment of in vivo murine cardiac metabolism, morphology, and function at physiological heart rates. Am J Physiol Heart Circ Physiol 279:H2218–H2224
50. Naumova AV, Weiss RG, Chacko VP (2003) Regulation of murine myocardial energy metabolism during adrenergic stress studied by in vivo 31P NMR spectroscopy. Am J Physiol Heart Circ Physiol 285:H1976–H1979
51. Omerovic E, Basetti M, Bollano E, Bohlooly M, Tornell J, Isgaard J, Hjalmarson A et al. (2000) In vivo metabolic imaging of cardiac bioenergetics in transgenic mice. Biochem Biophys Res Commun 271:222–228
52. Weidensteiner C, Horn M, Fekete E, Neubauer S, von Kienlin M (2002) Imaging of intracellular sodium with shift reagent aided (23)Na CSI in isolated rat hearts. Magn Reson Med 48:89–96
53. Ruff J, Wiesmann F, Lanz T, Haase A (2000) Magnetic resonance imaging of coronary arteries and heart valves in a living mouse: techniques and preliminary results. J Magn Reson 146:290–296
54. Manka DR, Gilson W, Sarembock I, Ley K, Berr SS (2000) Noninvasive in vivo magnetic resonance imaging of injury-induced neointima formation in the carotid artery of the apolipoprotein-E null mouse. J Magn Reson Imaging 12:790–794
55. Choudhury RP, Aguinaldo JG, Rong JX, Kulak JL, Kulak AR, Reis ED, Fallon JT et al. (2002) Atherosclerotic lesions in genetically modified mice quantified in vivo by non-invasive high-resolution magnetic resonance microscopy. Atherosclerosis 162:315–321
56. Hockings PD, Roberts T, Galloway GJ, Reid DG, Harris DA, Vidgeon-Hart M, Groot PH et al. (2002) Repeated three-dimensional magnetic resonance imaging of atherosclerosis development in innominate arteries of low-density lipoprotein receptor-knockout mice. Circulation 106:1716–1721
57. Itskovich VV, Choudhury RP, Aguinaldo JG, Fallon JT, Omerhodzic S, Fisher EA, Fayad ZA (2003) Characterization of aortic root atherosclerosis in ApoE knockout mice: high-resolution in vivo and ex vivo MRM with histological correlation. Magn Reson Med 49:381–385
58. Wiesmann F, Szimtenings M, Frydrychowicz A, Illinger R, Hunecke A, Rommel E, Neubauer S et al. (2003) High-resolution MRI with cardiac and respiratory gating allows for accurate in vivo atherosclerotic plaque visualization in the murine aortic arch. Magn Reson Med 50:69–74
59. Chaabane L, Soulas EC, Contard F, Salah A, Guerrier D, Briguet A, Douek P (2003) High-resolution magnetic resonance imaging at 2 Tesla: potential for atherosclerotic lesions exploration in the apolipoprotein E knockout mouse. Invest Radiol 38:532–538
60. Ahn D, Cheng L, Moon C, Spurgeon H, Lakatta EG, Talan MI (2004) Induction of myocardial infarcts of a predictable size and location by branch pattern probability-assisted coronary ligation in C57BL/6 mice. Am J Physiol Heart Circ Physiol 286:H1201–H1207
61. Nahrendorf M, Wiesmann F, Hiller KH, Han H, Hu K, Waller C, Ruff J et al. (2000) In vivo assessment of cardiac remodeling after myocardial infarction in rats by cine-magnetic resonance imaging. J Cardiovasc Magn Reson 2:171–180
62. Waller C, Hiller KH, Kahler E, Hu K, Nahrendorf M, Voll S, Haase A et al. (2001) Serial magnetic resonance imaging of microvascular remodeling in the infarcted rat heart. Circulation 103:1564–1569
63. Itter G, Jung W, Juretschke P, Schoelkens BA, Linz W (2004) A model of chronic heart failure in spontaneous hypertensive rats (SHR). Lab Anim 38:138–148
64. Nahrendorf M, Hu K, Fraccarollo D, Hiller KH, Haase A, Bauer WR, Ertl G (2003) Time course of right ventricular remodeling in rats with experimental myocardial infarction. Am J Physiol Heart Circ Physiol 284:H241–H248

65. Wiesmann F, Frydrychowicz A, Rautenberg J, Illinger R, Rommel E, Haase A, Neubauer S (2002) Analysis of right ventricular function in healthy mice and a murine model of heart failure by in vivo MRI. Am J Physiol Heart Circ Physiol 283:H1065–H1071
66. Nahrendorf M, Hiller KH, Theisen D, Hu K, Waller C, Kaiser R, Haase A et al. (2002) Effect of transmyocardial laser revascularization on myocardial perfusion and left ventricular remodeling after myocardial infarction in rats. Radiology 225:487–493
67. Hu K, Gaudron P, Anders HJ, Weidemann F, Turschner O, Nahrendorf M, Ertl G. (1998) Chronic effects of early started angiotensin converting enzyme inhibition and angiotensin AT1-receptor subtype blockade in rats with myocardial infarction: role of bradykinin. Cardiovasc Res 39:401–412
68. Nahrendorf M, Frantz S, Hu K, von zur Muhlen C, Tomaszewski M, Scheuermann H, Kaiser R et al. (2003) Effect of testosterone on post-myocardial infarction remodeling and function. Cardiovasc Res 57:370–378
69. Nahrendorf M, Hu K, Hiller KH, Galuppo P, Fraccarollo D, Schweizer G, Haase A et al. (2002) Impact of hydroxymethylglutaryl coenzyme a reductase inhibition on left ventricular remodeling after myocardial infarction: an experimental serial cardiac magnetic resonance imaging study. J Am Coll Cardiol 40:1695–1700
70. Reffelmann T, Hale SL, Dow JS, Kloner RA (2003) No-reflow phenomenon persists long-term after ischemia/ reperfusion in the rat and predicts infarct expansion. Circulation 108:2911–2917
71. Lund GK, Higgins CB, Wendland MF, Watzinger N, Weinmann HJ, Saeed M (2001) Assessment of nicorandil therapy in ischemic myocardial injury by using contrast-enhanced and functional MR imaging. Radiology 221:676–682
72. Watzinger N, Lund GK, Higgins CB, Chujo M, Saeed M (2002) Noninvasive assessment of the effects of nicorandil on left ventricular volumes and function in reperfused myocardial infarction. Cardiovasc Res 54:77–84
73. Saeed M, Watzinger N, Krombach GA, Lund GK, Wendland MF, Chujo M, Higgins CB (2002) Left ventricular remodeling after infarction: sequential MR imaging with oral nicorandil therapy in rat model. Radiology 224:830–837
74. Yang Z, Cerniway RJ, Byford AM, Berr SS, French BA, Matherne GP (2002) Cardiac overexpression of A1-adenosine receptor protects intact mice against myocardial infarction. Am J Physiol Heart Circ Physiol 282:H949–H955
75. Yang Z, Bove CM, French BA, Epstein FH, Berr SS, DiMaria JM, Gibson JJ et al. (2002) Angiotensin II type 2 receptor overexpression preserves left ventricular function after myocardial infarction. Circulation 106:106–111
76. Li B, Li Q, Wang X, Jana KP, Redaelli G, Kajstura J, Anversa P (1997) Coronary constriction impairs cardiac function and induces myocardial damage and ventricular remodeling in mice. Am J Physiol 273:H2508–H2519
77. Capasso JM, Jeanty MW, Palackal T, Olivetti G, Anversa P (1989) Ventricular remodeling induced by acute nonocclusive constriction of coronary artery in rats. Am J Physiol Heart Circ Physiol 257:H1983–H1993
78. Waller C, Hiller K-H, Albrecht M, Hu K, Nahrendorf M, Gattenlohner S, Haase A et al. (2003) Microvascular adaptation to coronary stenosis in the rat heart in vivo: a serial magnetic resonance imaging study. Microvasc Res 66:173–182
79. Schlieper G, Kim JH, Molojavyi A, Jacoby C, Laussmann T, Flogel U, Godecke A et al. (2004) Adaptation of the myoglobin knockout mouse to hypoxic stress. Am J Physiol Regul Integr Comp Physiol 286:R786–R792
80. Braun A, Trigatti BL, Post MJ, Sato K, Simons M, Edelberg JM, Rosenberg RD et al. (2002) Loss of SR-BI expression leads to the early onset of occlusive atherosclerotic coronary artery disease, spontaneous myocardial infarctions, severe cardiac dysfunction, and premature death in apolipoprotein E-deficient mice. Circ Res 90:270–276
81. Woodman SE, Park DS, Cohen AW, Cheung MW, Chandra M, Shirani J, Tang B et al. (2002) Caveolin-3 knock-out mice develop a progressive cardiomyopathy and show hyperactivation of the p42/44 MAPK cascade. J Biol Chem 277:38988–38997
82. Parzy E, Fromes Y, Wary C, Vignaux O, Giacomini E, Leroy-Willig A, Carlier PG (2003) Ultrafast multiplanar determination of left ventricular hypertrophy in spontaneously hypertensive rats with single-shot spin-echo nuclear magnetic resonance imaging. J Hypertens 21:429–436
83. Zou Y, Yamazaki T, Nakagawa K, Yamada H, Iriguchi N, Toko H, Takano H et al. (2002) Continuous blockade of L-type Ca2+ channels suppresses activation of calcineurin and development of cardiac hypertrophy in spontaneously hypertensive rats. Hypertens Res 25:117–124
84. Al-Shafei AI, Wise RG, Gresham GA, Bronns G, Carpenter TA, Hall LD, Huang CL (2002) Non-invasive magnetic resonance imaging assessment of myocardial changes and the effects of angiotensin-converting enzyme inhibition in diabetic rats. J Physiol 538:541–553
85. Al-Shafei AI, Wise RG, Gresham GA, Carpenter TA, Hall LD, Huang CL (2002) Magnetic resonance imaging analysis of cardiac cycle events in diabetic rats: the effect of angiotensin-converting enzyme inhibition. J Physiol 538:555–572
86. Johansson L, Johnsson C, Penno E, Bjornerud A, Ahlstrom H (2002) Acute cardiac transplant rejection: detection and grading with MR imaging with a blood pool contrast agent-experimental study in the rat. Radiology 225:97–103
87. Kanno S, Wu YJ, Lee PC, Dodd SJ, Williams M, Griffith BP, Ho C (2001) Macrophage accumulation associated with rat cardiac allograft rejection detected by magnetic resonance imaging with ultrasmall superparamagnetic iron oxide particles. Circulation 104:934–938
88. Jelicks LA, Chandra M, Shtutin V, Petkova SB, Tang B, Christ GJ, Factor SM et al. (2002) Phosphoramidon treatment improves the consequences of chagasic heart disease in mice. Clin Sci (Lond) 103 Suppl 48:267S–271S
89. Jelicks LA, Chandra M, Shirani J, Shtutin V, Tang B, Christ GJ, Factor SM et al. (2002) Cardioprotective effects of phosphoramidon on myocardial structure and function in murine Chagas' disease. Int J Parasitol 32:1497–1506
90. Huang H, Yanagisawa M, Kisanuki YY, Jelicks LA, Chandra M, Factor SM, Wittner M et al. (2002) Role of cardiac myocyte-derived endothelin-1 in chagasic cardiomyopathy: molecular genetic evidence. Clin Sci (Lond) 103(Suppl 48):263S–266S
91. Huang H, Chan J, Wittner M, Jelicks LA, Morris SA, Factor SM, Weiss LM et al. (1999) Expression of cardiac cytokines and inducible form of nitric oxide synthase (NOS2) in *Trypanosoma cruzi*-infected mice. J Mol Cell Cardiol 31:75–88